# Transparent thin film transistors using optimized oxide active layers and gate insulator

F. GHERENDI[*]

*National Institute for Lasers, Plasma and Radiation Physics (NILPRP), Plasma Physics and Nuclear Fusion Laboratory, L 22, P.O. Box MG-36, 077125, Magurele-Bucharest, Romania*

Transparent thin film transistors (TTFT) in "top gate – bottom contacts" geometry were built using high conductivity $In_2O_3$ for the source-drain contacts, respectively highly resistive $In_2O_3$ as channel layer. The pulsed electron beam deposition (PED) method was used for growing the $In_2O_3$ thin films. $Al_2O_3$ and $Y_2O_3$ thin films grown by reactive RF magnetron sputtering in different conditions were studied in order to obtain an optimized gate film for the TTFT.

## 1. Introduction

Transparent electronics is already present in current applications such as displays, intelligent windows and solar cells. Conducting transparent thin films is one of the main objects of study for making transparent circuitry, and amorphous In, Ga, Zn –oxides or mixtures in various proportions are used as thin films grown at room temperature in most applications [1-5].

Transparent electronic devices also require thin films with different electrical properties. Semiconductor films are also needed, and In – Ga – Zn -oxides can also play this role when the concentration of oxygen vacancies is reduced [6].

For making field effect transparent thin films transistors (TTFT) or capacitors, a high-k insulator film is needed in order to have a high gate capacitance, enabling the transistor to work at low gate voltage [7]. Some oxides, like $Al_2O_3$ and $Y_2O_3$, are of particular interest due to their high breakdown field strength [7, 8], alowing to increase the gate capacitance by reducing the gate film thickness. The quality of the insulator film has a crucial importance over the performances of the TTFT [6, 7], and optimization studies are needed in order to reduce leakage currents and cracks that would reduce the breakdown field strength and even result in pre-breakdown [8].

Large scale applications require the films to be grown at the room temperature [1, 4] and amorphous state of the film, which can be obtained at room temperature, is desired, because it determines higher carrier mobility for conducting/semiconductor thin films [4] as compared to the polycrystalline state.

Magnetron sputtering or chemical methods are suitable for growing thin films for large scale applications [1, 4, 6]. In opposition to magnetron sputtering, ablation methods are better in keeping the film stoichiometry unaltered compared to the target, faster and lower cost for

small scale applications [9-14], and therefore suitable for laboratory scale models.

The present study aims to optimize the insulator film grown by reactive RF magnetron sputtering for the gate insulator of a TTFT. A TTFT using $In_2O_3$ films grown by PED at room temperature as channel layer and source-drain contacts was built as laboratory model in order to evaluate the performances of the optimized insulator film.

## 2. Experimental setup

The pulsed electron deposition method (PED) [9, 15, 16, 17], is an ablation technique similar to pulsed laser deposition (PLD), but using a pulsed electron beam instead of the laser beam. The PED device, described in detail in previous works [17, 18], uses a pulsed capillary discharge to produce the pulse electron beam used for the ablation of the target. The PED method is well suited for growing transparent materials as for example high quality ZnO [16], ITO [14] and $In_2O_3$ thin films [17] with a good surface morphology.

The $In_2O_3$ thin films are grown by PED in pure oxygen, at low pressure for obtaining highly conducting source, drain and gate contacts, and at higher pressure for obtaining the channel film.

Transistors with the geometry presented in fig. 1 were made on an optical glass 12x25mm rectangular substrate. In the first step, working with the PED device at low oxygen pressure, the source and drain contacts were patterned with a mechanical shadow mask. A wire of 300μm diameter, part of the shadow mask, determines the channel length. The channel width was determined by the shape of the source and drain contacts. In a second step, the channel was grown by PED at a higher oxygen pressure. The extent of the channel film was limited by deposing it with a second mechanical shadow mask with a rectangular hole.

The third step in making the TTFT was the growth of the gate insulator thin film, using the optimized RF magnetron deposition, with another mechanical shadow mask, in order to leave access to the source and drain contacts.
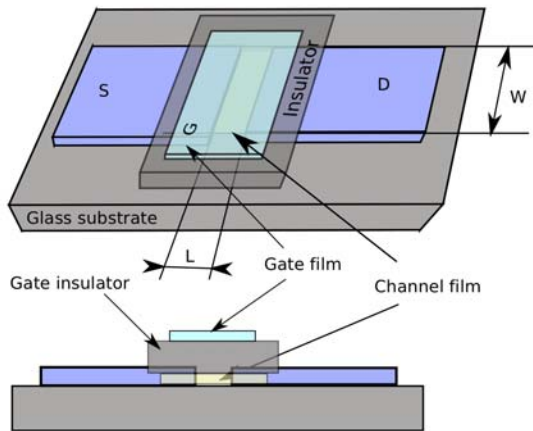


*Fig. 1. Structure of the top gate-bottom contacts TTFT .*

A preliminary study for optimizing the electrical properties of the insulator film was performed. RF magnetron sputtering in a Tectra (Germany) deposition system was used for growing $Al_2O_3$ and $In_2O_3$ test films. Oxygen was added to the sputtering argon in order to achieve reactive sputtering. The working RF power, gas pressure and oxygen percentage were varied, and the performances of the resulting films were compared. An ISO-TECH capacimeter with working frequency of 100kHz was used for measuring the dielectric constant, and a Keithley 2611A SourceMeter System for measuring the leakage current density and breakdown field.

The gate contacts were grown on top of the insulator film, using the same shadow mask that was used for patterning the channel. Aluminum deposited by resistive heating vapor deposition, as well as PED grown conductive $In_2O_3$ films were tested as gate contacts.

"Witness" $In_2O_3$ thin films were simultaneously grown with the source-drain and channel films in order to measure the carrier mobility of the $In_2O_3$ film by Hall effect measurements. A MMR Technologies H-50 Hall effect measurement system was used for this purpose.

The electrical characteristic curves of these transistors were measured with two Keithley 2611A SourceMeter systems linked by the Keithley TSP protocol.

## 3. Results

### 3.1. Electrical characteristics of the insulator

The leakage current density and breakdown strength was studied for $Al_2O_3$ and $Y_2O_3$ thin films grown by reactive RF magnetron sputtering in various conditions.

The films were deposited at room temperature. The deposition was performed in different $Ar:O_2$ mixture proportions, on commercial highly conductive ITO covered glass substrates. The optical transmittance of all these films was better than 85%. Several aluminum contact pads, 3 mm diameter, were deposited by resistive heating evaporation on top of the insulator films, and current-voltage characteristics were measured between them and the ITO layer, on several contacts, for statistics. The electrical field-current density curves were traced in order to obtain a better comparison between different films, considering that the thickness and the contact size may differ.

The $Al_2O_3$ films were grown by the RF magnetron sputtering technique, in pure Ar, determining an optimal pressure of $5 \times 10^{-3}$ mbar for which the deposition rate is convenient and the field strength of the film is sufficient for using it as a gate insulator in a TTFT. As shown in [8], adding oxygen to the working gas did not improve the quality of the film; however, as in the mentioned study, 1h target conditioning by dummy discharge in pure oxygen was necessary. An optimal deposition power of 200W was determined, for which a 150nm thick film is obtained after 6h deposition time.
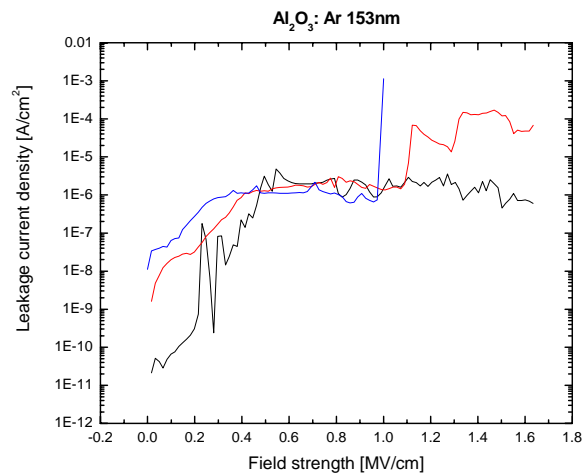


*Fig. 2: Leakage current density and breakdown field strength curves for $Al_2O_3$ thin films grown in pure Ar (measurements on 3 contact pads)*

In fig. 2 it can be seen that for a 168nm thickness the leakage current density of the $Al_2O_3$ films remains below $10^{-6}$ $A/cm^2$ at field strengths below 1MV/cm, for most of the tested contact pads. Such a current density would determine a gate current smaller than 1nA for a TTFT with a gate surface smaller than $1mm^2$. Dielectric breakdown of the film was observed at electric fields above 1MV/cm for measurements on most contact pads .

The dielectric constant of the film was determined from capacitance measurements between the aluminum contact pads and the ITO layer, resulting a value of about 8, typical for $Al_2O_3$ films [8].

The $Y_2O_3$ films were grown by sputtering at the same RF power of 200W. As shown in figure 3, 175nm thick $Y_2O_3$ thin films grown in pure Ar have leakage current densities smaller than $10^{-8}$ A/cm$^2$ on the non-breakdown region. The leakage is lower than for $Al_2O_3$ films, but the breakdown field strength is in average 0.5MV/cm, smaller than in the case of $Al_2O_3$ films.
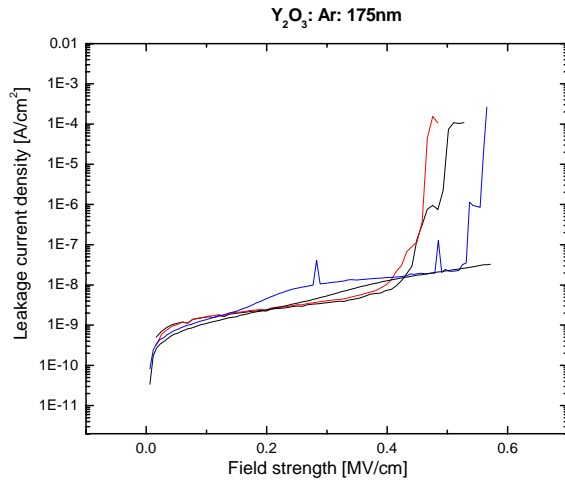
**$Y_2O_3$: Ar: 175nm**



*Fig. 3. Leakage current density and breakdown field strength curves for $Y_2O_3$ thin films grown in pure Ar (measurements on 4 contact pads).*

Adding $O_2$ to the Ar background gas in RF magnetron deposition dramatically decreases the deposition rate. While the film grown in pure Ar had 175nm thickness, adding 6% $O_2$ resulted in a 70nm thin film after 6h deposition time.

The leakage current curves (fig. 4) shown very dispersed statistics compared to the film grown in pure Ar, and even a decrease of the average breakdown strength to 0.4 MV/cm. However, the leakage current densities of around $10^{-7}$ A/cm$^2$ are quite low for a film thickness of only 70nm.
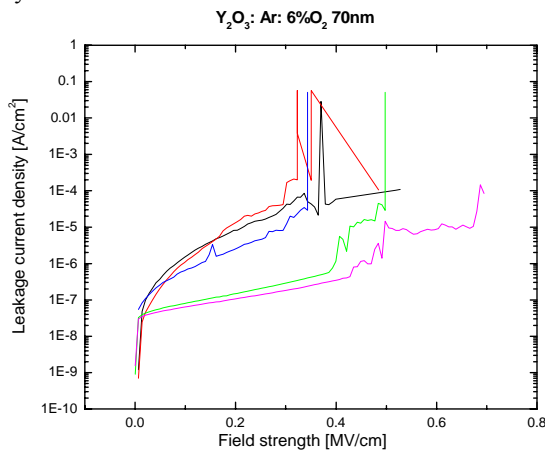
**$Y_2O_3$: Ar: 6%$O_2$ 70nm**



*Fig. 4. Leakage current density and breakdown field strength curves for $Y_2O_3$ thin films grown in Ar:6%$O_2$*
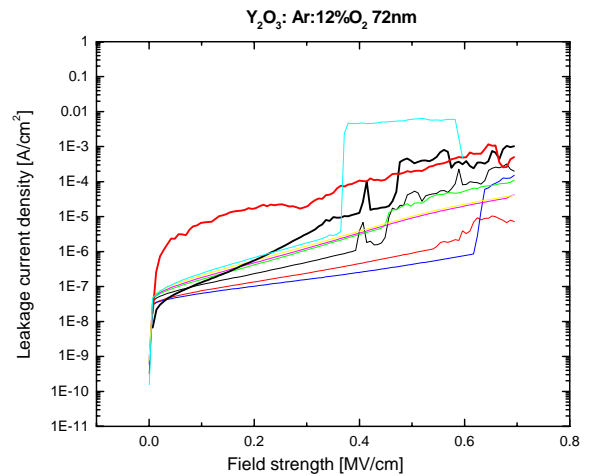
**$Y_2O_3$: Ar:12%$O_2$ 72nm**



*Fig. 5. Leakage current density and breakdown field strength curves for $Y_2O_3$ thin films grown in Ar:12%$O_2$*

Increasing the oxygen pressure at 12% and keeping the same growth conditions, the deposition rate does not decrease more, the resulting film having 72nm thickness after 6h.

As shown in figure 5, these films have better statistics of leakage currents, a slightly lower leakage current density at practically the same film thickness as for the films grown in 6 % $O_2$, but the most important, average breakdown field strength higher than 0.6MV/cm, better than in the case of the films grown in pure Ar.

The capacitance per unit area of the $Y_2O_3$ films was $C_{ox} \approx 160$ nF/cm$^2$, resulting into a dielectric constant of about 20, with practically no dependence on the argon-oxygen composition.

Based upon the results presented above, putting into balance the dielectric constant (a larger value allowing to obtain higher gate capacitance for thicker film) and the breakdown field strength, $Y_2O_3$ films grown with 12% oxygen were used as gate insulator for the TTFT.

### 3.2. Characteristics of the TTFT

The source, drain and gate contacts of the TTFT were grown by PED at an oxygen pressure of $1.3 \times 10^{-2}$ mbar. In order to measure the electrical characteristics of the gate, source and drain contacts, "witness" $In_2O_3$ thin films were grown in the same deposition process. These films are highly transparent and conductive, with a Hall mobility of the carriers of 47cm$^2$/Vs, carrier density of $2.2 \times 10^{20}$ cm$^{-3}$ and a resistivity $6 \times 10^{-4}$ Ω cm, matching our previous experiments [17, 19, 20]. As described in the literature [6], this high conductivity is mainly due to the oxygen vacancies.

The TTFT channel was grown by PED at higher oxygen pressure ($2 \times 10^{-2}$ mbar). Measurements on the witness film reveal a pure semiconductor behavior with a carrier Hall mobility of ~24 cm$^2$/Vs and density of $2.5 \times 10^{14}$cm$^{-3}$, and a resistivity as high as $10^3$ Ω cm**.**

The TTFT that we have built has a channel length of 300μm and a channel width of 2mm. The $In_2O_3$ channel film has a thickness of ~80nm and the $Y_2O_3$ gate insulator has a thickness of ~110nm.

The transfer characteristic curve of such a TTFT for a 4V drain-source voltage is presented in figure 6. This curve reveals an enhanced mode TTFT.

The maximum on/off current ratio measured from this curve is $4 \times 10^4$. The "off" leakage current equals the gate current, which is of the order of tens to hundreds of picoamperes.

The subthreshold swing, calculated from the slope of the linear portion of the curve in Fig. 6 left axis, is about 0.6V/decade, value comparable to those reported in literature [6, 5].
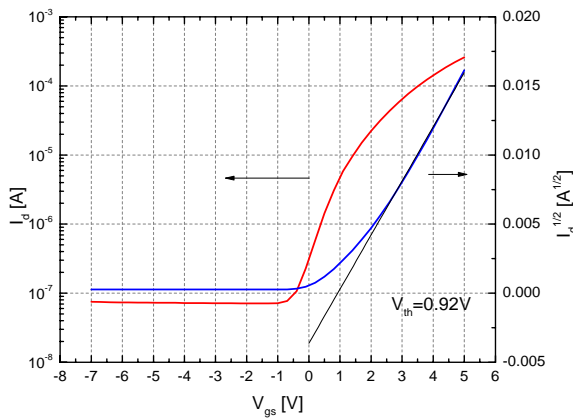


Fig.6: Transfer characteristic curve $(I_d(V_{gs}))$ of the TTFT

The threshold voltage was determined using the plot of the square root of the drain current in function of the gate voltage (Fig. 6 right axis). The value determined for the threshold voltage, by extrapolating the linear portion towards the zero of the current, was +0.92V.

A family of output characteristics of the same transistor is presented in figure 7, showing saturation $V_{ds}$ voltages in the range 2 to 3.5V, and a saturation current of ~850μA for $V_{gs}=+3V$.

The drain current in the saturation regime, as given in [6], is

$$I_d = \frac{\mu_{nsat}C_{ox}}{2}\frac{W}{L}\left(V_{gs}-V_{th}\right)^2\left(1+\lambda\left(V_{ds}-V_{dssat}\right)\right) \quad (1)$$

where $\mu_{nsat}$ is the saturation carrier mobility in the channel, $C_{ox}$ is the capacitance per unit area of the gate insulator oxide film, W and L are the channel width and length, λ is a parameter related to the channel length and channel modulation that determines the slope of the current characteristics in the saturation region (see curves in figure 7) and $V_{dssat}$ is the drain saturation voltage.
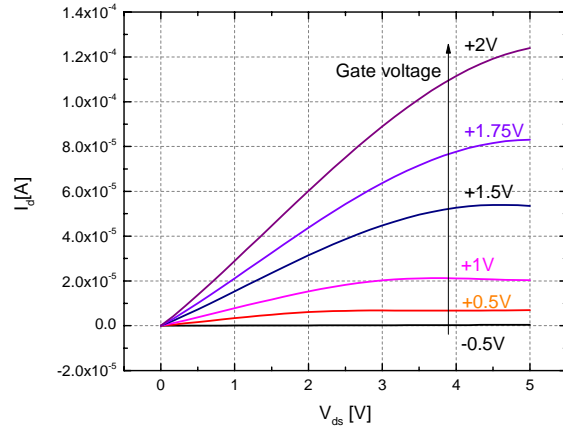


Fig. 7. Output characteristics family $(I_d(V_{ds}))$ of the TTFT for gate voltages between -0.5 and +2V.

From (1), using the slope of the square root of the drain current (fig.6 right axis) we determined the saturation carrier mobility of the channel $\mu_{nsat} \approx 19cm^2/Vs$ in the gate voltage range of -0.5 to 0V. This value is very close to the mobility of the carriers determined by Hall effect on the witness films grown simultaneously with the channel films.

The measured optical transmittance of the $Y_2O_3/In_2O_3$ TTFT is between 75 and 85% in the visible range, glass substrate included, that means 80-90% without the glass substrate. The cut-off wavelength is around 300-350 nm (the cut-off wavelength of the optical glass substrate is 280 nm).

## 4. Conclusions

An optimization study for the gate insulator thin films grown by RF magnetron sputtering was performed in order to obtain a film with the best balance between a high breakdown field strength and a small leakage current density. $Al_2O_3$ and $Y_2O_3$ thin films grown by reactive RF magnetron sputtering in various $Ar:O_2$ mixtures were studied. The best breakdown performances were observed for $Al_2O_3$ films, but the $Y_2O_3$ films have better leakage performance and higher dielectric constant (~20 vs. ~8). The $Y_2O_3$ films grown in 12% oxygen have higher breakdown field strength than $Y_2O_3$ films grown at lower oxygen pressure, at comparable leakage currents, and therefore are better gate insulators.

An enhanced mode TTFT was fabricated using $In_2O_3$ thin films grown by PED as active layers (channel and source-drain contacts) and the optimized $Y_2O_3$ thin film as gate insulator. The electrical characteristics of the TTFT are: subthreshold swing of 0.6V/dec, a threshold voltage of 0.92V, saturation current of 850μA, on/off ratio of $4 \times 10^4$ and saturation channel mobility of $19cm^2/Vs$. The transparency of the TTFT is better than 80% in the visible range.

## Acknowledgements

## References

[1] H. Hosono, Thin Solid Films **515**, 6000 (2007)

[2] R.L. Hoffman, B.J. Norris, J.F. Wager, Appl. Phys. Lett. **82** (5), 733 (2003)

[3] E.M.C. Fortunato, P.M.C. Barquinha, A.C.M.B.G. Pimentel, A.M.F. Goncalves, A.J.S. Marques, R.F.P. Martins, L.M.N. Pereira, Appl. Phys. Lett. **85**(13), 2541 (2004)

[4] R. Martins, E. Fortunato, P. Barquinha, L. Pereira, Transparent Electronics: From Materials to Devices, Wiley-Blackwell, ISBN 978-0470683736 (2012)

[5] P. F. Carcia, Application of Transparent Oxide Semiconductors for Flexible Electronics, in Transparent Electronics: From Synthesis to Applications, Ed. By A.Facchetti ans T.Marks, Wiley & Sons Ltd ISBN 978-0-470-99077-3, p.271 (2010)

[6] J. F. Wager, D. A. Keszler, R. E. Presley, Transparent Electronics, Springer, ISBN 978-0-387-72341-9 (2008)

[7] G. Adamopoulos, S. Thomas, D. C.Bradley, M. A. McLachlan, T. D. Anthopoulos, Appl. Phys. Lett. **98**, 123503 (2011)

[8] M. Voigt, M. Sokolowski, Mat. Sci. Eng. B **109**, 99-103 (2004).

[9] S. Tricot, N. Semmar, L. Lebbah, C. Boulmer-Leborgne, Journal of Physics D: Applied Physics **43**, 065301 (2010)

[10] E. Le Boulbar, E. Millon, J. Mathias, C. Boulmer-Leborgne, J. Perrière, M. Nistor, F.Gherendi, N. Sbaï, J. B.Quoirin, Appl. Surf. Sci. **257**, 5380 (2011)

[11] E. Millon, M. Nistor, C. Hebert, Y. Davila, J. Perrière, J. Mat. Chem. **22**, 12179 (2012)

[12] J. Gonzalo, C.N. Alfonso, F. Vega, D.M. Garcia, J. Perriere, Appl. Surf. Sci. **86**, 40 (1995)

[13] M. Nistor, A. Ioachim, B. Gallas, D. Defourneau, J. Perrière, W. Seiler, J. Phys. Cond. Matt. **19,** 096006, pp. 1-16 (2007)

[14] M. Nistor, A. Petitmangin, C. Hebert, W. Seiler, Appl. Surf. Sci. **257**, 5337 (2011)

[15] M. Nistor, P. Charles, M. Ganciu, M. Lamoureux, N. B. Mandache, A.M. Pointu, Plasma Sources Sci. Technol. **11**, 183(2002)

[16] S. Tricot, M. Nistor, E. Millon, C. Boulmer-Leborgne, N.B. Mandache, J. Perrière and W. Seiler, Surf. Sci. **604** (21-22), 2024 (2010)

[17] W. Seiler, M.Nistor, C.Hebert, J.Perrière, Solar Energy Materials & Solar Cells **116**, 34 (2013)

[18] M. Nistor, F. Gherendi, N.B. Mandache, Appl. Surf. Sci. **258** (23), 9274 (2012)

[19] F. Gherendi, M. Nistor, S. Antohe, L. Ion, I. Enculescu, N.B. Mandache, Semicond. Sci. Technol. **28** (8), 085002 (2013)

[20] F. Gherendi, M. Nistor, N.B. Mandache, J. Displ. Tech **9**(9), 760 (2013)

_____

Corresponding author: florin.gherendi@infim.ro